Orbital
The electronic journal of chemistry

the electronic journal of chemistry

Full Paper | http://dx.doi.org/10.17807/orbital.v13i1.1582

Theoretical Study of Tautomeric Conformations for 1,2,4-Triazole Derivatives

Radia Mahboub*

We have performing theoretical calculations of the 1,2,4-triazole derivatives using DFT B3LYP method to study the tautomeric conformations of 1,2,4-triazole-3-thiol (TL 2A and TL 2C) and 1,2,4-triazole-3-thione (TL 2B) derivatives. Then, we compare the obtained results to methyltriazole thioether (MTE 1). The full geometry optimizations were carried out using 6-31G basis set. The frontier orbital energy, atomic net charges were discussed.

Graphical abstract

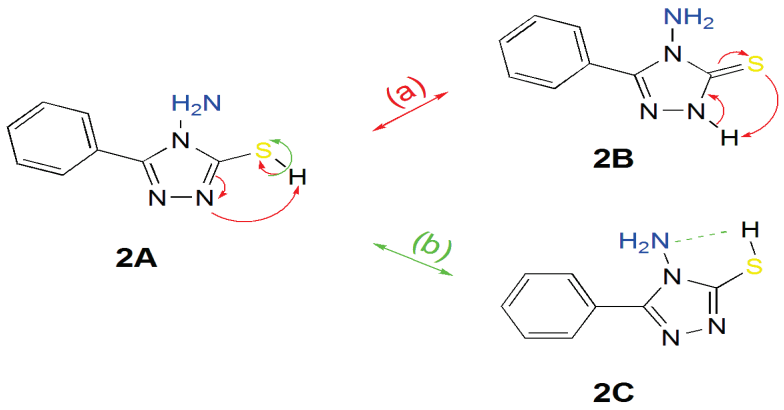

Keywords

1,2,4-Triazole
Tautomeric conformations
Methylthioether
Theoretical calculations

Article history

Received 13 December 2020
Revised 01 February 2021
Accepted 04 February 2021
Available online 13 March 2021

Editor: Valdemar Lacerda Júnior

1. Introduction

Triazole derivatives have attracted a large number of scientists. Triazoles are used as analytical reagent [1], dye [2] and in the preparation of polymers [3]. Their important applications appear in the fields of medicine [4, 5] agriculture [6] and industry [7]. In 1885, Bladin was the first to synthesized 1,2,4-triazole derivatives [8, 9]. Recently, synthesis of 1,2,3-triazole has conducted via C-F bond cleavage [10]. Different methods have been used to prepare 1,2,4-triazole derivatives. The best known are Pellizzari and Einhorn-Brunner reactions [11]. Authors have used various series of compounds as: i) carboxylic acid hydrazide [12], ii) 1,3,5-triazine [13], iii) oxazole [14], iv) thiosemicarbazide [15], v) urea [16] and vi) acid chloride [17] for preparing 1,2,4-triazoles. Numerous bioactive sulfur-related 1,2,4-triazole have been reported for their different activity, such as antibacterial [18, 19], anti-tumor [20], anti-HIV [21], and anti-TMV [22]. The C-substituted 1,2,4-triazoles have been widely studied experimentally and computationally in many areas for their tautomeric equilibrium. The tautomeric equilibrium of substituted 1,2,4-triazoles has been widely studied to elucidate the influence of the substituents attached to the triazole ring or introduced on the phenyl ring linked to the triazole. The tautomers effects affect the reactivity of compounds in chemical processes as: alkylation, acylation and nucleophilic substitution; biological and biochemical systems through their equilibrium. Tautomerism is important for many biological and biochemical processes. It is an essential factor which can modify the properties of nucleic acids. As a result, the adoption of a tautomeric form may influence the bioactivity of potential new drugs [23-29].

Department of Chemistry, Faculty of Sciences, University of Tlemcen, B.P. 119, Tlemcen, 13 000, Algeria. *Corresponding author. E-mail: **radiamahboub@yahoo.com**

In the present paper, we have evaluated the performance of DFT B3LYP method in the study of the tautomeric conformations of some 1,2,4-triazole derivatives : 4-amino-5-phenyl-4*H*-1,2,4-triazole-3-thiol 2A, 4-amino-5-phenyl-2*H*-1,2,4-triazole-3-thione 2B, and 4-amino-5-phenyl-4*H*-1,2,4-triazole-3-thiol 2C (respectively TL 2A, TN 2B and TL 2C) then to compared the obtained results to 4-amino-3-methylthio-5-phenyl-4*H*-1,2,4-triazole 1 (MTE 1) (Fig. 1).

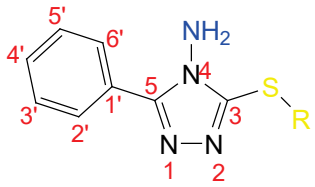

1: R = Me

2: R = H

Fig. 1. Structures of 1,2,4-triazoles.

2. Results and Discussion

Our objective was to study the following tautomers: 4-amino-5-phenyl-4*H*-1,2,4-triazole-3-thiol 2A [30, 11] 4-amino-5-phenyl-2*H*-1,2,4-triazole-3-thione 2B, and 4-amino-5-phenyl-4*H*-1,2,4-triazole-3-thiol 2C (respectively TL 2A, TN 2B and TL 2C) then to compared the obtained results to 4-amino-3-methylthio-5-phenyl-4*H*-1,2,4-triazole 1 (MTE 1) [31]. For the last compound, we have chosen the most stable conformation which correspond to the *cis*-form (with torsion angle $\Phi 1_{(N4\text{-}C3\text{-}S\text{-}Me)}$ = 180°).

The thiol group has two properties. The TL 2A structure can exchange the proton with nitrogen in position 2 and give thione TN 2B. Thus, the stability of the tautomer depends on the conjugation and the resonance of the structures. Furthermore, the thiol group can rotate freely and leads to the existence of two tautomers TL 2A and TL 2C. The two tautomers have specific conformations with different torsion angles (TL 2A: $\Phi 1_{(N4\text{-}C3\text{-}S\text{-}H)}$ = 180°, $\Phi 2_{(N2\text{-}C3\text{-}S\text{-}H)}$= 0°; TL 2C: $\Phi 1_{(N4\text{-}C3\text{-}S\text{-}H)}$ = 0°, $\Phi 2_{(N2\text{-}C3\text{-}S\text{-}H)}$= 180°) (Fig. 2).

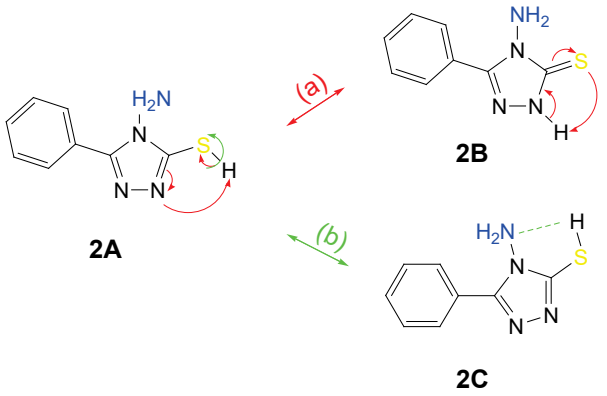

Fig. 2. Tautomeric conformations: of 4-amino-5-phenyl-2*H*-1,2,4-triazole-3-thione TN 2B, and 4-amino-5-phenyl-4*H*-1,2,4-triazole-3-thiols: TL 2A and TL 2C.

From the DFT B3LYP method, we have evaluated: i) frontier molecular orbital (HOMO and LUMO), ii) chemical hardness (η), iii) electrophilicity index (ω) and iv) fraction of electrons *ΔN*. These results are listed in Table 1. Based on the frontier molecular orbital theory, HOMO and LUMO are the most important factors which can affect the reactivity of molecule. The energy gap (EG) between the HOMO and LUMO describes an important stability factor [32-34].

Our simulated results reveal that the tautomer thione TN 2B has a high reactivity if compared to that of MTE 1 and relative to TL 2A and TL 2C (Table 1, entry 6). In contrast, the chemical hardness η of TL 2A is higher than that to tautomer TL 2C and thionic form TN 2B (Table 1, entry 7). The TL 2C conformation results from the formation of intramolecular hydrogen bond S-H···NH_2. Thus, this molecule adopts a pseudo-five hydrazinylmethanethiol ring. At the opposite, we note that the electrophilicity index ω increases with electrophilic power of a molecule (TN 2B) and withdrawing effect of nitrogen in the intramolecular hydrogen bond (TL 2C) (Table 1, entry 10).

We conclude that this equilibrium is shifted towards the most stable tautomer following the order TN 2B> TL2A> TL2C. As a result, the thionic form is predominant and may influence receptor activity.

Table 1. Quantum chemical parameters for different triazoles with DFT B3LYP method.

Entry	Parameter	MTE 1	TL 2A	TN 2B	TL 2C
1	E_t (eV)	-26282.493	-25212.895	-259.311	-25212.822
2	μ (D)	4.311	4.697	3.686	7.588
3	IP (eV)	5.922	6.149	5.768	6.177
4	HOMO (eV)	-5.922	-6.149	-5.768	-6.177
5	LUMO (eV)	-1.106	-1.056	-1.415	-1.252
6	EG (eV)	4.816	5.093	4.353	4.925
7	η (eV)	2.408	2.546	2.176	2.463
8	σ (eV^{-1})	0.415	0.393	0.460	0.406
9	χ (eV)	3.514	3.603	3.591	3.714
10	ω (eV)	2.564	2.550	2.966	2.800
11	$\Delta N_{(110)}$	0.271	0.239	0.289	0.224

The fraction of electrons *ΔN* transferred between inhibitor molecules and the metal surface can be estimated according to the following equations 1 and 2 [35, 36]:

$$\Delta N_{(110)} = \frac{(\chi_{met} - \chi_{inh})}{2(\eta_{inh} + \eta_{met})} \quad (1)$$

$$\Delta N_{(110)} = \frac{(\Phi_{Fe_{(110)}} - \chi_{inh})}{2\eta_{inh}} \quad (2)$$

where $\Phi_{Fe_{(110)}}$ = 4.82 Ev is the metal work function used rather than χ_{Fe}, more suitable for an adsorbate-metal surface interaction and high stability [35, 37], and η_{Fe} = 0.

Table 1 shows that all the ΔN values calculated for the interaction between the inhibitory molecules and the $Fe_{(110)}$ surface are positive. This result indicates that all these molecules have the ability to donate electrons to the vacant orbital d of the metal (Fe). Thus, calculated ΔN values of the inhibitors decrease by the order of TN 2B > MTE 1 > TL 2A > TL 2C, which allows a better capacity for adsorption of TN 2B on metal surface. Accordingly, the fraction of electrons ΔN correlate very well with those of the energy gap values given over (Table 1, entries 6, 11). The transfer of electron is hardly increases by the presence of thione form (TN 2B), the introduction of thioether group on the 1,2,4-triazole ring (MTE 1) and the non steric hindrance of the thiol tautomers (TL 2A and TL 2C) (Fig. 3).

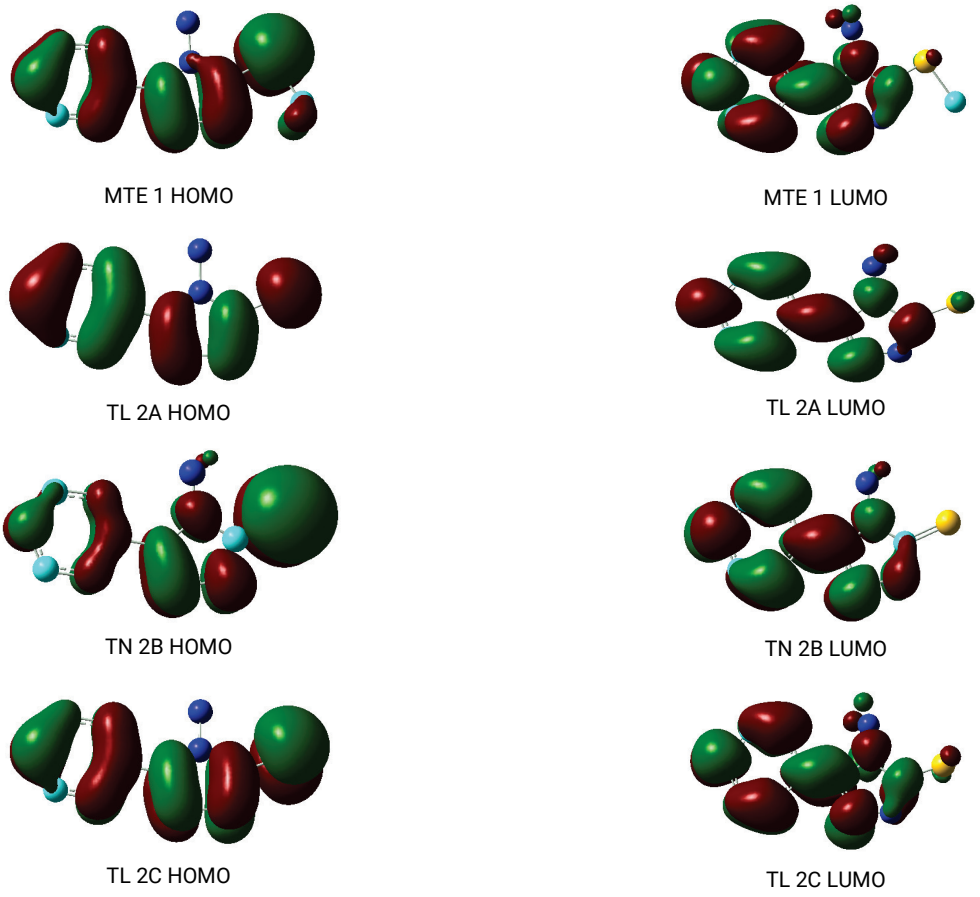

Fig. 3. Frontier molecular orbitals (HOMO and LUMO) of MTE 1, TL 2A, TN 2B and TL 2C. Hydrogens are omitted for clarity.

The calculated Mulliken charge distributions of the different triazoles distributions are shown in Fig. 4. The Mulliken charges of these molecules occur due to polarization on each compound. All nitrogen atoms are negatively charged. The Mulliken charges on nitrogen atom N_4 is more negative than that on NH_2, N_1 and N_2. In TN 2B tautomer, the nitrogen atom N_2 is the most negative due to the neighboring atom C_3 charged positively. Within the triazole thione, S is negative this is due to the resonance (C = S) while in the three molecules are positive (S-H, S-Me). All aromatic carbon atoms are negatively charged except $C_{1'}$ due to its bonding with the triazol ring. C_5 is the highest positively charged carbon atom due to it bonding to nitrogens. The hydrogen atoms are located at different functional group such as amine, thiol, methyl and phenyl. Thus, all hydrogen atoms are positively charged.

Molecular electrostatic potential (MESP) is an important tool for studying the relationship between molecular structure and chemical property. Each 2D ESP representation drawn as an outline around each molecule is an MESP surface. The external contour has a lower iso-surface value and the internal contour has a higher iso-surface value. The surface of the electrostatic potential (ESP) indicates the available unoccupied surface around the molecule where the excitation is going to reside around the molecule. It gives the molecular size, the shape and the distribution of the charges [38, 39].

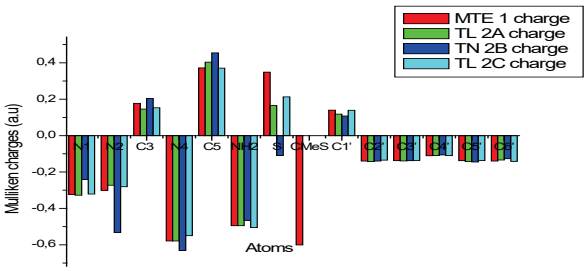

Fig. 4. Mulliken charge distribution for different triazoles.

First, we used MESP as a visual method to evaluate the relative polarity of each molecule. Thus, the different values of the electrostatic potential are represented by different colors; blue, red and green. The potential increases in the following order: blue> green> yellow> orange> red. We note that the negative region (red, orange and yellow) indicates

the electrophilic reactivity for: i) the nitrogen atoms N1 and N2 (in the triazole group) for MTE 1, TL 2A and TL 2C molecules, and ii) the sulfur atom for TN 2B tautomer while the positive region (blue) reveals the nucleophilic reactivity of the NH_2 amine group of all these compounds.

To complete this study, we also used the electrostatic potential (ESP). The negative regions are associated to: nitrogen atoms in amine and triazole groups for TL 2A and TL 2C tautomers. In thionic form TN 2B, the situation is different. The negative regions are associated to: nitrogen atoms in amine group and imine bond (included in triazole) and sulfur atom in thione function. The proton of the thiol group is exchanged on the nitrogen located in alpha of the thione function by prototropy phenomenon, and transformed into a secondary amine. Therefore, it loses its nucleophilic reactivity.

For the compound MTE 1, the situation is identical to that TL 2A and TL 2C conformers. Concerning the nitrogen atom in triazole, the difference is situated in thioether function which interacts with amino group. The electrostatic potentials of nitrogen atoms in triazole, amine groups, imine bond and thione function ranging from -4 to -40 10^{-3} a. u. has been unchanged in compounds MTE 1, TL 2A, TN 2B and TL 2C.

We conclude that compound TN 2B has the highest polarity. The 2D representation of electrostatic potential (ESP), molecular electrostatic potential map (MESP) and 3D electrostatic potential (ESP) surface of triazoles are illustrated in Fig. 5.

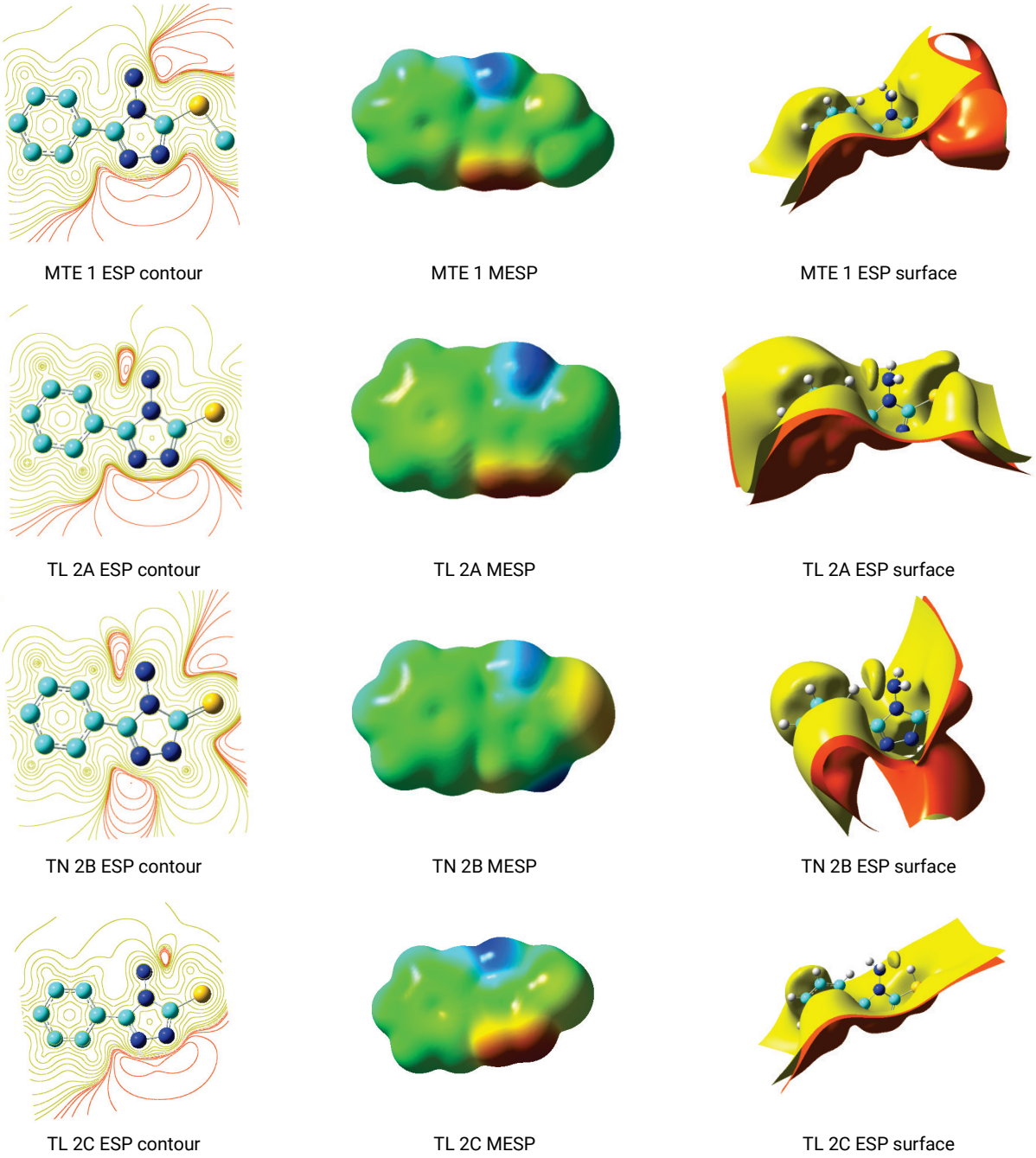

Fig. 5. Electrostatic Potential (ESP) contour, Molecular Electrostatic Potential map (MESP) and Electrostatic potential (ESP) surface of triazoles. Hydrogens are omitted for clarity (iso-value 0.0004).

3. Material and Methods

The molecular quantum optimisation calculations are performed by density functional theory DFT B3LYP method using 6-31G basis set implemented in Gaussian 03 W programme [40-43]. The following quantum chemical results are considered: total energy (E_t), ionisation potential (IP), energy of the highest occupied molecular orbital (E_{HOMO}), energy of the lowest unoccupied molecular orbital (E_{LUMO}), energy gap (EG = E_{LUMO} - E_{HOMO}), dipole moment (μ), chemical hardness (η = - (E_{LUMO} - E_{HOMO})/2), softness (σ = 1/η), Mulliken electronegativity (χ = - (E_{LUMO} + E_{HOMO})/2), electrophilicity index (ω = χ^2/2η) [44], and the fraction of electrons (ΔN = ($\Phi_{Fe(110)}$-χ_{inh}) /2η_{inh}) [35, 36].

4. Conclusions

We have studied the tautomeric form of 4-amino-5-phenyl-4*H*-1,2,4-triazole-3-thiol 2A, 4-amino-5-phenyl-2*H*-1,2,4-triazole-3-thione 2B, and 4-amino-5-phenyl-4*H*-1,2,4-triazole-3-thiol 2C (respectively TL 2A, TN 2B and TL 2C) then we compared the obtained results to 4-amino-3-methylthio-5-phenyl-4*H*-1,2,4-triazole 1 (MTE 1). The simulated results reveal that the tautomer thione 2B has a high reactivity than MTE 1. We note also that the electrophilicity index ω increases with electrophilic power of a molecule. MTE 1 and TL 2A have similar electrophilicity index. However, TL 2C has a high value due to intramolecular hydrogen bond. The transfer of electron is hardly increased by the presence of thione form (TN 2B). This result correlates very well with this of the energy gap value.

Molecular electrostatic potential (MESP) shows that the electrophilic reactivity is located on the thione group, while the nucleophilic reactivity is situated on N1, N2 and NH_2. We conclude that compound TN 2B has the highest polarity. The Mulliken analyses explicate the net charge distribution of the computed molecules.

From the obtained data, we suggest that tautomer TN 2B is the preferred and stable form of resonance; TL 2A and TL 2C are the most stable tautomeric forms strongly depend on the orientation of thiol group. We conclude that 4-amino-5-phenyl-2*H*-1,2,4-triazole-3-thione 2B and 4-amino-3-methylthio-5-phenyl-4*H*-1,2,4-triazole 1 (MTE 1) have big capacity to transfer electrons to a metal surface. The predicted results indicated that 1,2,4-triazoles with thione and thioether functions can be considered as best corrosion inhibitors.

References and Notes

[1] Busch, M. *Ber. Dtsch. Chem. Ges*. **1905,** *38*, 856. [Crossref]

[2] Nakaic, T.; Meedu, S.; Kurahashi, T. Jpn Pat 73:89932 1973. (CA 81: 65182).

[3] Colter, R. J.; Matzner, M. Ring Terming Polymerisation, Part-B-1. Heterocyclic Ring, Academic. New York, 1972.

[4] Prasad, A. T.; Ramalingam, R. J.; Rao, A. B.; Diwan, P. V.; Sattur, P. B. *Eur. J. Med. Chem*. **1989**, *24*, 199. [Crossref]

[5] Bayrak, H.; Demirbas, A.; Bektas, H.; Demirbas, N.; Alpay-Karaoglu, S.; Demirbas, N. *Turk. J. Chem.* **2010**, *34*, 835. [Crossref]

[6] Mu, J-X.; Zhai, Z-W.; Tan, C-X.; Weng, J-Q.; Wu, H-K.; Duke, SO.; Zhang, Y-G.; Liu, X-H. *J. Heterocyclic. Chem*. **2019**, *56*, 968. [Crossref]

[7] Kashyap, A.; Silakari, O. Triazoles: Multidimensional 5-Membered Nucleus for Designing Multitargeting Agents, 208; pp323-342. Key Heterocycle Cores for Designing Multitargeting Molecules, Ed; Om Silakari, 2018, Chap 9. [Crossref]

[8] Bladin, J. A. *Ber. Dtsch. Chem. Ges*. **1885**, *18*, 666. [Crossref]

[9] Singh, A. K.; Kandel, K. R. *J. Nepal. Chem. Soc.* **2012**, *30*, 174. [Crossref]

[10] Zhou, Q.; Fu, Z.; Yu, L.; Wang, J. *Asian. J. Org. Chem.* **2019**, *8*, 646. [Crossref]

[11] Kaur, P.; Kaur, R.; Goswami, M. *Int. Res. J. Pharm.* **2018**, *9*, 1. [Crossref]

[12] Bayrak, H.; Demirbas, A.; Demirbas, N.; Karaoglu, S. A. *Eur. J. Med. Chem.* **2009**, *44*, 4362. [Crossref]

[13] El-Reedy, A. A. M.; Soliman, N. K. *Sci. Rep*. **2020**, *10*, 6137. [Crossref]

[14] Askar, F. W.; Hassan, H. A.; Jinzeel, N. A. *Baghdad. Sci. J.* **2013**, *10*, 766. [Crossref]

[15] Hashim, C. S.; Alias, M. F. *Baghdad. Sci. J.* **2012**, *9*, 668. [Crossref]

[16] K-Kaymakcioglu, B.; Celen, A. O.; Tabanca, N.; Ali, A.; Khan, S. I.; Khan, I. A.; Wedge, D. E. *Molecules* **2013**, *18*, 3562. [Crossref]

[17] El Ashry, E. S. H.; Kassem, A. A.; Abdel-Hamid, H.; Louis, F. F.; Khattab, S. A. N.; Aouad, M. R. *Arkivoc* **2006**, *14*, 119. [Crossref]

[18] Dilmaghani, K. A.; Pur, F. N.; Jazani, N. H.; Alavi, A.; Niknam, Z.; Mirfakhraee, F. *Phosphorus Sulfur Silicon Relat. Elem*. **2014**, *189*, 81. [Crossref]

[19] Plech, T.; Wujec, M.; Kosikowska, U.; Malm, A. *Lett. Drug. Des. Discov.* **2013**, *10*, 917. [Crossref]

[20] Kaldrikyan, M. A.; Melik-Oganjanyan, R. G.; Aresnyan, F. H. *Pharm. Chem. J.* **2013**, *47*, 191. [Crossref]

[21] Zia, M.; Akhtar, T.; Hameed, S.; Al-Masoudi, N. A. *Z. Naturforschung B* **2012**, *67*, 747. [Crossref]

[22] Xiong, Q. Z.; Lin, X. F.; Liu, J. H.; Bi, L.; Bao, X. P. *Chin. J. Org. Chem.* **2012**, *32*, 1255. [Crossref]

[23] Nagy, P. I.; Tejada, F. R.; Messer, W. S. *J. Phys. Chem. B* **2005**, *109*, 22588. [Crossref]

[24] Ozimiński, W. P.; Dobrowolski, J-Cz.; Mazurek, A. P. *J. Mol. Struct.* **2004**, *680*, 107. [Crossref]

[25] Kubota, S.; Uda, M. *Chem. Pharm. Bull*. **1975**, *23*, 955. [Crossref]

[26] Palmer, M. H.; Christen, D. *J. Mol. Struct.* **2004**, *705*, 177. [Crossref]

[27] Bojarska-Olejnik, E.; Stefaniak, L.; Witanowski, M.; Webb, G. A. *Magn. Reson. Chem.* **1986**, *24*, 911. [Crossref]

[28] Karpińska, G.; Dobrowolski, J-Cz. *Comput. Theor. Chem.* **2015**, *1052*, 58. [Crossref]

[29] Dolzhenko, A. V.; Pastorin, G.; Dolzhenko, A. V.; Chui, W. K. *Tetrahedron Lett.* **2009**, *50*, 2124. [Crossref]

[30] Sahoo, P. K.; Sharma, R.; Pattanayak, P. *Med. Chem.*

Res. **2010**, *19*, 127. [Crossref]

[31] Oshima, T.; Niwa, Y.; Kuwata, K.; Srivastava, A.; Hyoda, T.; Tsuchiya, Y.; Kumagai, M.; Tsuyuguchi, M.; Tamaru, T.; Sugiyama, A.; Ono, N. ; Zolboot, N. ; Aikawa, Y. ; Oishi, S. ; Nonami, A. ; Arai, F.; Hagihara, S.; Yamaguchi, J.; Tama, F.; Kunisaki, Y.; Yagita, K.; Ikeda, M.; Kinoshita, T.; A. Kay, S.; Itami, K. ; Hirota, T. *Sci. Adv.* **2019**, *5*, eaau9060. [Crossref]

[32] Pearson, R. G. *J. Org. Chem.* **1989**, *54*, 1423. [Crossref]

[33] Zhou, Z.; Parr, R. G. *J. Am. Chem. Soc.* **1990**, *112*, 5720. [Crossref]

[34] Faust, W. L. *Science* **1989**, *245*, 37. [Crossref]

[35] Haque, J.; Srivastava, V.; Chauhan, D. S.; Lgaz, H.; Quraishi, M. A. *ACS. Omega* **2018**, *3*, 5654. [Crossref]

[36] Kokalj, A. *Faraday. Discuss.* **2015**, *180*, 415. [Crossref]

[37] Saha, S. Kr.; Murmu, M.; Murmu, N. C.; Banerjee, P. *J. Mol. Liq.* **2016**, *224*, 629. [Crossref]

[38] Zhang, Z.; Tian, N. C.; Huang, X. D.; Shang, W.; Wu, L. *RSC. Adv.* **2016**, *6*, 22250. [Crossref]

[39] Murray, S.; Politzer, P. *Comput. Mol. Sci.* **2011**, *2*, 153. [Crossref]

[40] Frisch, M. J.; Trucks, G. W.; Schlegel, H. B.; Scuseria, G. E.; Robb, M. A.; Cheeseman, J. R.; Montgomery, J. A.; Vreven, Jr. T.; Kudin, K. N.; Burant, J. C.; Millam, J. M.; Iyengar, S. S.; Tomasi, J.; Barone, V.; Mennucci, B.; Cossi, M.; Scalmani, G.; Rega, N.; Petersson, G. A.; Nakatsuji, H.; Hada, M.; Ehara, M.; Toyota, K.; Fukuda, R.; Hasegawa, J.; Ishida, M.; Nakajima, T.; Honda, Y.; Kitao, O.; Nakai, H.; Klene, M.; Li, X.; Knox, J. E.; Hratchian, H. P.; Cross, J. B.; Adamo, C.; Jaramillo, J.; Gomperts, R.; Stratmann, R. E.; Yazyev, O.; Austin, A. J.; Cammi, R.; Pomelli, C.; Ochterski, J. W.; Ayala, P. Y.; Morokuma, K.; Voth, G. A.; Salvador, P.; Dannenberg, J. J.; Zakrzewski, V. G.; Dapprich, S.; Daniels, A. D.; Strain, M. C.; Farkas, O.; Malick, D. K.; Rabuck, A. D.; Raghavachari, K.; Foresman, J. B.; Ortiz, J. V.; Cui, Q.; Baboul, A. G.; Clifford, S.; Cioslowski, J.; Stefanov, B. B.; Liu, G.; Liashenko, A.; Piskorz, P.; Komaromi, I.; Martin, R. L.; Fox, D. J.; Keith, T.; Al-Laham, M. A.; Peng, C. Y.; Nanayakkara, A.; Challacombe, M.; Gill, P. M. W.; Johnson, B.; Chen, W.; Wong, M. W.; Gonzalez, C.; Pople, J. A. Gaussian 03, Revision C.02, Gaussian, Inc., Wallingford CT, 2004.

[41] Becke, A. D. *J. Chem. Phys.* **1993**, *98*, 5648. [Crossref]

[42] Becke, A. D. *Phys. Rev. A* **1988**, *38*, 3098. [Crossref]

[43] Lee, C.; Yang, W.; Parr, R. G. *Phys. Rev. B* **1988**, *37*, 785. [Crossref]

[44] Parr, R. G.; Szentpaly, L. V.; Liu, S. *J. Am. Chem. Soc.* **1999**, *121*, 1922. [Crossref]

How to cite this article

Mahboub, R. *Orbital: Electron. J. Chem.* **2021**, *13*, 33.
http://dx.doi.org/10.17807/orbital.v13i1.1582